Article

Incipient Inter Turn Short Circuit Fault Detection on Induction Motors Through Data Fusion and Statistical Machine Learning Strategy

Arturo Yosimar Jaen-Cuellar [1], David Alejandro Elvira-Ortiz [1] and Juan Jose Saucedo-Dorantes [1,*]

[1] Engineering Faculty, San Juan del Rio Campus, Autonomous University of Queretaro, Rio Moctezuma 249, San Juan del Rio, Querétaro, Mexico, 76807; arturo.yosimar.jaen@uaq.mx (A.Y.J.-C.); david.elvira@uaq.mx (D.A.E.-O).

* Correspondence: juan.saucedo@uaq.mx (J.J.S.-D.).

Abstract: The new technological developments have allowed the evolution of the industrial process to this new concept called industry 4.0, which integrates power machines, robotics, smart sensors, communication systems, and internet of things to have more reliable automation systems. However, the electrical rotating machines like the Induction Motor (IM) is still widely used in several industrial applications since their robust elements, high efficiency, and versatility in industrial applications. Nevertheless, the occurrence of faults in IMs is inherent to their operating conditions, hence, Inter-turn short-circuit (ITSC) is one of the most common failures that affect IMs and its appearance is due to electrical stresses leads to the degradation of the stator winding insulation. In this regard, this work proposes a diagnosis methodology for the assessment and detection of incipient ITSC in IMs, the proposed method is based on the processing of vibration, stator currents and magnetic stray-flux signals. Certainly, the novelty and contribution include the characterization of different physical magnitudes by estimating a set of statistical time domain features, as well as, their fusion and reduction through the Linear discriminant Analysis technique within a feature-level fusion approach. Furthermore, the fusion and reduction of information from different physical magnitudes leads to perform the automatic fault detection and identification by a simple Neural-Network (NN) structure. The proposed method is evaluated under a complete set of experimental data and the obtained results demonstrate that the fusion of information from different sources (physical magnitudes) allows to improve the accuracy during the detection of ITSC in IMs, the results make this proposal feasible to be incorporated as a part of condition-based maintenance programs in the industry.

Keywords: condition monitoring, induction motor, inter-turn short-circuit, machine learning, statistical features

1. Introduction

In recent years, the advent of the industry 4.0 has been possible due to the evolution of the technologies together with the integration of advanced communication systems [1,2] and smart sensors [3]. Despite this technological growth, the induction motor (IM) remains as the medullar column to provide to the industrial processes with mechanical rotative power, linear motion, and to propel mechanisms in general [4]. The typical applications of this machine are as pumps, fans, compressors, manufacturing, materials processing, refrigeration, transportation, conveyors, shredders, etc., [5]. The electrical rotating machines are electromechanical systems used in industry because of its benefits such as low cost, high efficiency, high output torque ratio, high power to weight ratio, easiness of maintenance, reliability, applicability, low noise emissions, among others [6,7]. According to the reported literature, the induction machines are one of the most common and widespread motors over the globe in industry, constituting around the 80% from the total industrial equipment [8], and they consume approximately between the 40% and the 80%

 doi:10.20944/preprints202306.0180.v1

of the total energy generated for these companies [9–11]. Therefore, considering this information, any industrial process downtime due to motor failures would impact directly in aspects like overall costs, maintenance planning, equipment damage or replacement, possibility of user risks or injuries, and even environmental effects (because energy consumed by IMs is generated majorly through conventional fuels) [12]. Now, typically the ensemble of an IM considers several components that allow its proper operations being the principal ones the stator, the rotor, the windings, the rolling bearings, and the fan [13]. Recently, several scientific reviews have analyzed and concluded that, in relation with the motor components the most typical faults and their corresponding percentages ranges of occurrence are the following [14–16]: bearing faults between 40% to 50%, stator winding faults between 28% to 38%, rotor related faults between 5% to 10%, and other associated faults between 12% to 28%. From previous information, it can be noted that the faults associated with the stator windings are the second major problems that appear in the components of the IM. But also, in turn, a specific failure related to the stator circuit are the inter-turn short-circuits (ITSC) faults [17] that affect the IM performance with high probability of severe equipment damage, and for this reason they are still a topic of interest.

Particularly speaking about the ITSC faults in electric rotative machines, in the literature much research has been carried out addressing this phenomenon. It has been reported that ITSC faults are the most common and frequent electrical problems, and they represent approximately between 30% and 40% of all types of stator circuit damages [18]. These faults are understood as damage in the winding insulation and they can occur at different locations of the coil turns in a single phase [19]. The general circumstances that cause failures in the electric motors are harsh environments at industry like high temperatures, humidity, mechanical tension due to overloads, contamination, grease, vibrations, electric discharges and over voltages, among others [20]. However, for the particular case of the ITSC the causes are, for example, flows of current with an intensity that exceeds the nominal operating conditions, generating in consequence a release of energy in the form of heat and mechanical stress, or the use of fast switching PWM inverters that accelerates the insulation degradation [19,21]. Some effects of the ITSC faults in the motors are of course malfunctioning on its operation, performance reduction, local magnetic saturation, asymmetric behavior of the motor, to mention some [20,22]. With the purpose of better understand the inter-turn short circuits, several investigations have developed models of these faults, such as the case of the finite element models (FEM) [18,23], parametric mathematical models based on electrical circuits [24,25], and combined FEM-parametric models [26,27]. The objective of such models is the development of methodologies for detecting such faults in simulation environments, but assuming or omitting other conditions that could happen in real systems.

Regarding the classical methodologies, there exist several works that have developed approaches addressing ITSC detection. For example, in [6] the implementation of an improved wavelet packet transform (WPT) was done over the rotor current and the motor vibration signals in LabVIEW for permanent magnet synchronous motors (PMSM). In other works, like in [28], a Kalman filter excludes the frequency components corresponding to the 3rd, 5th, and 7th harmonics in the current signal measured from an IM, then the time-frequency spectrogram of the signal is used to obtain a gray level image and its corresponding histogram. With this information, the considerable deviations of the histograms distributions from a normal distribution are used for the detection of the ITSC. On the other hand, some works focused their efforts on the development of methodologies based on non-intrusive signal like magnetic flux in motor for detecting ITSC faults. Such as the case of the research in [29], that present a statistical methodology for detecting ITSC faults that uses a correlation coefficient between two external magnetic field signals measured by two sensors located symmetrically in the motor vicinity. The correlation obtained is based on the Pearson correlation coefficient applied on induction and synchronous machines. In this same area, the approach described in [30] also makes use of non-invasive stray magnetic field sensors for discriminating ITSC on salient pole synchronous generators (SPSG). To achieve the discrimination of the fault, the system model is developed by

 doi:10.20944/preprints202306.0180.v1

means of finite element method (FEM), and by introducing a unique pattern observed on the time-frequency domain signal processing through the short time Fourier transform (STFT). By its part, an online approach for detecting ITSC in PMSM is developed in [31] using stray magnetic field measured from the stator yoke. For this purpose, the inter-turn short-circuits dynamic, and the stray magnetic flux dynamic are implemented through FEM considering 24 sensitive tunneling magnetoresistive (TMR) sensor units. In other work, the harmonic analysis of different electric signal is performed in [32] for detecting ITSCs in the stator windings of squirrel cage IMs. The signals considered are stator phase current, external magnetic flux, and electromagnetic torque at different load levels. The validation of this proposal was through simulation by means of FEM. Meanwhile, in [33] is presented a methodology for diagnosing ITSC faults for line start PMSM through the frequency analysis of acoustic signals. The acoustic signals are decomposed through the fast Fourier transform (FFT) analyzing their amplitudes. It is worth mentioning that many works address the ITSC faults diagnosis on motors through infrared thermographic analysis, such as the work in [34] that develops an online non-intrusive algorithm which extracts features from the infrared histogram of the images profile taken from the hottest region of the machine surface. In this same line, the research in [35] describes an online non-invasive technique that detects the ITSC fault and its severity through two methods. The first method uses transient thermal monitoring during motor starting, and the second method implements pseudo coloring technique on infrared image of the motor on the steady state. On the same line, the work in [36] presents a methodology for diagnosing ITSC faults in the stator winding based on an infrared thermopile sensor array (IRSA) and a hall-effect sensor array (HESA). With these arrays direct contactless measurements of temperature and magnetic flux distribution along the end-winding region is done. Later, deviations in thermal and magnetic symmetries induced by the faults are assessed for detection. By its part, the work presented in [37] develops a metal-coated fiber Bragg grating (FBG) sensor to monitor the temperature and magnetic field around the end winding of IMs. The sensor measurements are decoupled by a filtering stage and the separated data is analyzed in the time-frequency domain for detecting the ITSC. From previous works discussion it is notorious the effort done for diagnosing the inter-turn short circuits on electric motors in what can be defined as classical ways acquiring signals and processing them by means of space transformations. However, they are mostly validated through model simulations omitting some real operating condition, and they do not consider data fusion to improve the detection reliability.

Recently, some methodologies addressed the use of data driven, machine learning, and deep learning techniques for detecting and diagnosing motor faults associated to ITSC with high accuracy. For example, an online fault detection framework is developed in [38] by collecting data from IMs, performing multiple extraction/selection of features, finding the most sensitive ones, and enhancing the classification task by integrating multiple classifiers. Meanwhile, in [39] a methodology for incipient ITSC diagnosis on PMSM based on data driven digital twins is described. For this purpose, a theoretical analysis of the three-phase current residuals under ITSC is carried out, and a digital twin model of a healthy target motor is defined through nonlinear auto-regressive model with exogenous inputs (NARX) network, at last the incipient faults are detected through current residual. Now, in relation to the machine learning (ML) approaches, several works have developed methodologies, such as in [40], where the support vector machines (SVM) and the convolutional neural networks (CNN) techniques are implemented for diagnosing ITSC on PMSM. In such work, it was demonstrated that SVM have more efficient training than CNN considering that the first technique requires much fewer data. In the same context, an developed algorithm combines the discrete wavelet transform (DWT) for multiresolution analysis (MRA), the statistical features extraction, and ML techniques, processes voltage signals generated by axial leakage flux from an IM for detecting incipient ITSC [41]. In other case, a fault diagnosis method applied on PMSM is presented in [42], where a sparse representation is used for extracting the first and second largest sparse coefficient of current and vibration signals, and for composing four-dimensional feature vectors.

Preprints (www.preprints.org) | NOT PEER-REVIEWED | Posted: 2 June 2023 doi:10.20944/preprints202306.0180.v1

Then, the feature vectors are input to the SVM for final diagnosis of ITSC, this is convenient for small samples sets. Similarly, the study presented in [43] explores the potential of several ML classifiers and the signal processing for the online condition monitoring of ITSC in the field winding of SPSG. In that work the data set for the ML is generated by applying the FFT on the power spectral density of the air gap magnetic field, DWT energies, and time series feature extraction based on hypothesis test. At last, but not least, the deep learning techniques are also present in the ITSC faults diagnosis. For instance, in [44] is described an approach based on the conditional generative adversarial net (CGAN) and an optimized sparse auto encoder (OSAE) applied on PMSM, an important attribute of this approach is the use of small samples sets. Other work explores the use of neural networks as efficient diagnosing tools for estimating the percentage of stator winding shorted turns on three-phase IMs. The implementation was done in MATLAB under different load conditions [45]. From the previous discussion of the works reported in the literature, it can be noted that data-driven, machine learning, and deep learning are techniques and schemes that provide reliable approaches for detecting ITSC. Mostly of them use the analysis of two measured signals, such as current and vibration, or current and stray magnetic flux form the motor. But it would be interesting to explore the potential of using currents, vibrations, and stray magnetic flux signals of different sensor channels (or sensor axes), perform features extraction, and make data fusion and classification.

The contribution of this work is with an integrated methodology based on a statistical machine learning strategy and data fusion of several physical signals measured from an induction motor for detecting the early occurrence of ITSC faults. At first place, the physical signals from the motor corresponding to the phase currents, the vibrations, and the external magnetic stray flux are acquired. Next, several statistical features are extracted from the time-domain signals to compose sets of sensitive matrices of features related to the fault condition, which will integrate a general high dimension matrix providing meaningful information about the fault not directly from the time-domain signals but considering its statistical data patterns. Posteriorly, a feature level fusion is carried out through the linear discriminant analysis, which will reduce the matrix of features of high dimensionality to a two-dimensional representation having those significant features for being used in the last classification stage. Finally, a classifier with simple structure based on the neural networks is implemented for performing the final diagnosis. The proposed methodology is capable of detecting different machine conditions, and for this case four conditions are considered: the healthy state of the motor and three fault conditions with different severities of ITSC (2, 4, and 6 coil turns in short circuit). The experimental tests considered the motor operation under four operating frequencies (15 Hz, 30Hz, 50Hz and 60Hz). The obtained results demonstrate the reliability and efficiency of the proposed methodology.

2. Materials and Methods

Electrical rotating machines like the induction motor (IM) is subjected to electrical stresses that can lead to the sudden occurrence of faults, in this sense, the stator inter-turn short-circuits (ITSC) are common faults caused by problems associated with the stator winding insulation. Consequently, an amplitude increase is produced in the harmonic component of the stator current signature when IMs are operating under the influence of ITSC, similarly, the air-gap flux density is also modified when ITSC occur. In this regard, classical approaches based on MCSA perform the detection of ITSC by analyzing the spectra of stator currents and/or magnetic stray-flux through Equation (1).

$$f_{ITSC} = f_s\left(k\frac{(1-s)}{p} \pm m\right) \quad (1)$$

Preprints (www.preprints.org) | NOT PEER-REVIEWED | Posted: 2 June 2023 doi:10.20944/preprints202306.0180.v1

Where f_s represents the supply frequency, s is the per unit slip, p is the pair of poles in the IM and k and m are integers that can be defined as $k = 1, 2, 3, \ldots$ and $m = 1, 3, 5, \ldots$

On the other side, although electrical problems such as ITSC produce direct affections over those electrical patterns like stator currents or magnetic stray flux, the abnormal appearance of vibrations is additionally produced since the magnetic field asymmetry being altered by the three-phase asymmetry of the IM windings. Theoretically, a characteristic fault-related vibrations frequency component of the stator appears at $2f_s$; moreover, the occurrence of vibrations due to ITSC leads also to characteristic harmonic components that can be located at $4f_s$ and $8f_s$ in a vibration spectrum. Accordingly, regardless that ITSC in IMs can be detected through different physical magnitudes like stator currents, magnetic flux and vibrations, the accurate assessment depends on the considered signal processing. Hence, processing techniques achieved in the time domain, frequency domain and time-frequency domain are commonly used to analyze signals and to extract characteristic fault-related patterns produced by the occurrence of faults.

Aiming to contribute to the field of condition monitoring and fault detection, in this work is proposed a diagnosis methodology for detecting the incipient occurrence of ITSC in IMs through the estimation of a set of statistical time-based domain features from different physical magnitudes such as stator currents, magnetic stray-flux and vibrations. Additionally, the computed statistical features are then pooled to carry out a feature-level fusion by means of the linear discriminant analysis (LDA) technique. Finally, the automatic identification of incipient ITSC in IMs is achieved by a proposed neural network (NN) classifier. The flow chart of the proposed method is shown in Figure 1 and consists of five main steps: i) Electromechanical pulley-belt system, ii) Data acquisition, iii) Feature calculation, iv) Feature fusion-reduction, and v) Automatic fault classification.

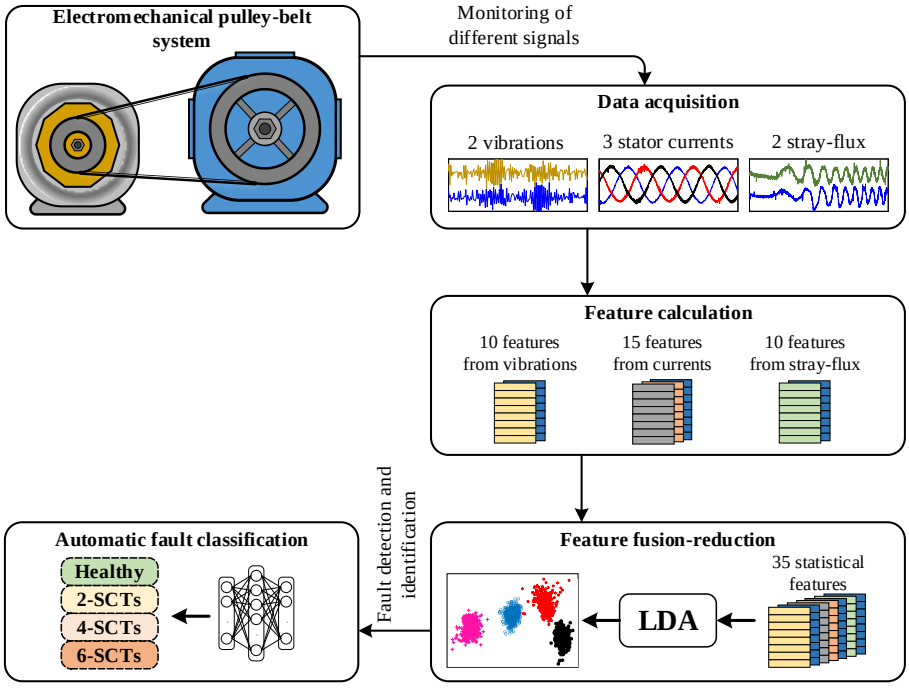

Figure 1. Flow chart of the proposed methodology based on the acquisition of different signals for identifying the incipient occurrence of ITSCs in IMs.

2.1. Electromechanical pulley-belt system

The electromechanical pulley-belt system is the system under evaluation and is composed by an IM coupled to an automotive alternator (AA) by means of a pulley-belt system. Particularly, in the IM are tested four different conditions comprising the healthy

Preprints (www.preprints.org) | NOT PEER-REVIEWED | Posted: 2 June 2023 doi:10.20944/preprints202306.0180.v1

state (HLT) and three incipient conditions of ITSC such as 2-SCTs, 4-SCTs and 6-SCTs. Each one of the aforementioned conditions is iteratively tested in the IM under different operating conditions in order to monitor its behavior through multiple sensors that allow the measurement of vibrations, stator currents, and magnetic stray flux.

2.2. Data acquisition

The data acquisition is carried out by a self-designed and proprietary data acquisition system (DAS) based on a field programmable gate array (FPGA), hence, the proprietary DAS allows the continuous monitoring of the IM operation by means of the measurement of vibrations, stator currents, and magnetic stray flux signals. Specifically, the vibrations are measured from the radial (V_r) and tangential (V_t) axes of the IM, the stator currents belong to the three lines currents (C_1, C_2 *and* C_3) of the IM, and the magnetic stray flux comprises the measurement of the axial (M_a) and radial (M_r) components. In this regard, for each performed test, the aforementioned signals are continuously recorded and stored in a personal computer for further analysis; moreover, the acquisition of the signals is carried out during 150 seconds of the continuous operation of the IM.

2.3. Feature calculation

The feature calculation is achieved with the aim of characterizing the previously acquired signals and it is mainly based on the estimation of a set of statistical time-domain features. The features calculation is individually applied to each one of the acquired signals, thereby, a signal $\mathbf{S}$ composed by n samples is first segmented into equal parts of one second, where every second of the signals has a length L as Equation (2) depicts:

$$\mathbf{S}_i = \left[\mathbf{S}_i^{1:L}, \mathbf{S}_i^{L+1:2L}, \dots, \mathbf{S}_i^{(((n/L)-1)n)+1:n}\right] \tag{2}$$

Once the signal segmentation is carried out, from each segmented part is estimated a meaningful set of five statistical time-domain features leading to obtain a characteristic feature matrix for each considered physical magnitude. Certainly, from the vibration signals are estimated $\mathbf{V_r} \in \mathbb{R}^{(5)}$ and $\mathbf{V_t} \in \mathbb{R}^{(5)}$ for the radial and tangential axis, respectively; from the stator signatures are estimated $\mathbf{C_1} \in \mathbb{R}^{(5)}$, $\mathbf{C_2} \in \mathbb{R}^{(5)}$ and $\mathbf{C_3} \in \mathbb{R}^{(5)}$ correspondingly for each current line and, from the axial and radial magnetic stray-flux components are estimated $\mathbf{M_a} \in \mathbb{R}^{(5)}$ and $\mathbf{M_r} \in \mathbb{R}^{(5)}$, respectively. The set of statistical time-domain features as well as the corresponding mathematical expressions are summarized in Table 1, Equations (3) to (7). These statistical features are proposed due to their capability to model trends, distributions, asymmetries, forms, dispersion, and changes in signals; additionally, their low computational cost can lead to quick responses when implemented.

Table 1. Considered set of statistical time-domain features for the characterization of the acquired signals.

Name	Mathematical equation	
Maximum value, $\hat{x} =$	$\hat{x} = max(x)$	(3)
Root mean square, x_{RMS}	$x_{RMS} = \sqrt{\frac{1}{n} \cdot \sum_{k=1}^{n} (x_k)^2}$	(4)
Standard deviation, x_σ	$x_\sigma = \sqrt{\frac{1}{n} \cdot \sum_{k=1}^{n} (x_k - \bar{x})^2}$	(5)
Shape factor, x_{SF}	$x_{SF} = \frac{\sqrt{\frac{1}{n} \cdot \sum_{k=1}^{n} (x_k)^2}}{\frac{1}{n} \cdot \sum_{k=1}^{n} \lvert x_k \rvert}$	(6)

Preprints (www.preprints.org) | NOT PEER-REVIEWED | Posted: 2 June 2023 doi:10.20944/preprints202306.0180.v1

Crest factor, x_{CF}	$x_{CF} = \frac{\hat{x}}{\sqrt{\frac{1}{n} \cdot \sum_{k=1}^{n} (x_k)^2}}$	(7)

Where x is the input vector of data; and x_k is the *k-th* individual sample.

2.4. Feature fusion-reduction

The feature fusion is performed within a feature-level fusion approach in which all previously estimated feature matrices ($\mathbf{V_r}$, $\mathbf{V_t}$, $\mathbf{C_1}$, $\mathbf{C_2}$, $\mathbf{C_3}$, $\mathbf{M_a}$ and $\mathbf{M_r}$) are then pooled into a single set. Thus, the single data set considers the fusion of information since all characteristic feature matrices are concatenated as Figure 2 shows. In this sense, it should be clarified that three global features matrices $\mathbf{V}$, $\mathbf{C}$ and $\mathbf{M}$ are considered for representing each one of the physical magnitudes within the feature-level fusion approach. Afterward, the pooled single data set $\left([\mathbf{V} \quad \mathbf{C} \quad \mathbf{M}] \in \mathbb{R}^{(35)}\right)$ are subsequently subjected to a reduction and space transformation procedure, in which, a new set of extracted features are obtained by means of applying the LDA techniques. The space transformation allows to achieve a dimensionality reduction from $\mathbb{R}^{(35)}$ to $\mathbb{R}^{(2)}$, in fact, the new achieved representation into the 2*D* space facilitates the visualization of all evaluated conditions due to the resulting features representing the linear combination (in different weights) of the original feature space.

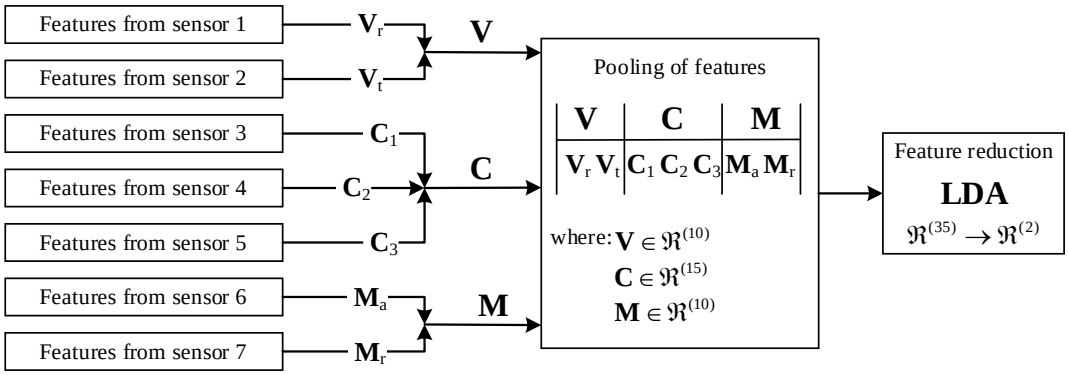

Figure 2. Representation of the feature-level fusion approach performed in this work for fusioning information from different physical magnitudes.

2.5. Automatic fault classification

The automatic fault classification of incipient ITSC in IMs is carried out by a NN-based classifier with a simple structure, the main objective of this stage is to evaluate the set of features extracted by the LDA technique. In this sense, the proposed NN classifier consists of three main layers such as input, hidden and output, where, the input layer is represented by two neurons in order to represent each one of the extracted features in the 2*D* space, the hidden layer has ten neurons as is recommended in the literature [46] and, four neurons in the output layer representing each one of the evaluated conditions. In addition, the NN-based classifier is trained and tested under a *five*-fold cross-validation scheme with the aim of obtaining statistically significant results, during the training are considered fifty epochs and a back-propagation algorithm. Moreover, the NN classifier considers a sigmoid function as the activation function allowing to evaluate the percentage of correspondence with each membership function in the output layer. A representation of the proposed NN structure is presented in Figure 3.

Preprints (www.preprints.org) | NOT PEER-REVIEWED | Posted: 2 June 2023 doi:10.20944/preprints202306.0180.v1

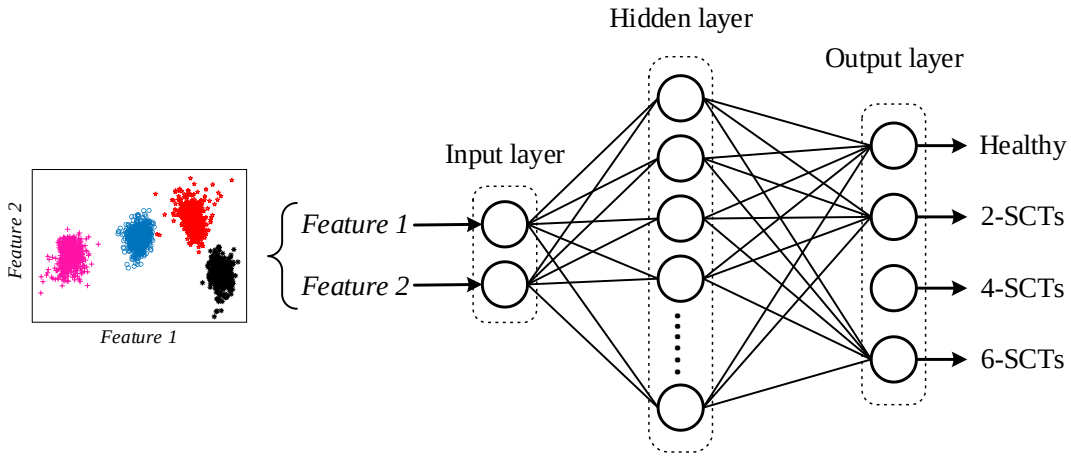

Figure 3. Schematic representation of the simple structure considered in the proposed NN-based classifier for carrying out the automatic fault detection and identification of incipient ITSCs in IMs.

3. Experimental test bench

In order to verify the performance of the proposed methodology for the detection of the incipient occurrence of ITSC in IMs, experimentation is performed using a 1.49kW (2HP) three-phase induction motor from WEG. The main specifications of the motor are summarized in the Table 2.

Table 2. Specifications of the 2HP WEG induction motor under test.

Specification	Value
Rated Power	1.49 kW
Rated Voltage	220 V
Rated Current	5.6 A
Pole Pairs	2

To feed the IM it is used a variable frequency drive (VFD) so the rotational speed can be controlled. In this work, a total of four different frequencies are achieved by using the VFD: 15 Hz, 30 Hz, 50 Hz and 60 Hz. This way it is possible to demonstrate the effectiveness of the proposed approach regardless the frequency of the power supply. Also, with the purpose of providing the motor with a load, it is coupled to a 12 V alternator by means of a pulley-belt system that represents between the 15% and the 25% of the nominal load. To produce the occurrence of ITSC in the IM, three different severities of ITSC are artificially induced in a single stator winding. The first severity considers 2-short circuit turns (2-SCTs), the second one 4-SCTs, whereas the third comprises 6-SCTs. Since the motor under test contains a total of 141 turns per phase winding, these severities represent 1.42%, 2.85% and 4.28% of damage, respectively. Therefore, a total of four operating conditions are assessed in this work: the healthy condition (HLT) and three ITSC severities (2-SCT, 4-SCT and 6-SCTs). Moreover, every condition is also tested using the four operating frequencies generated by means of the VFD (15 Hz, 30 Hz, 50 Hz and 60 Hz). To achieve the different ITSC severities, three taps are located at the points where the faults were induced. Each tap can be selected by closing a switch connected to an external resistor R_e so the short circuit current can be limited to avoid catastrophic damage of the motor (see Figure 4).

Preprints (www.preprints.org) | NOT PEER-REVIEWED | Posted: 2 June 2023 doi:10.20944/preprints202306.0180.v1

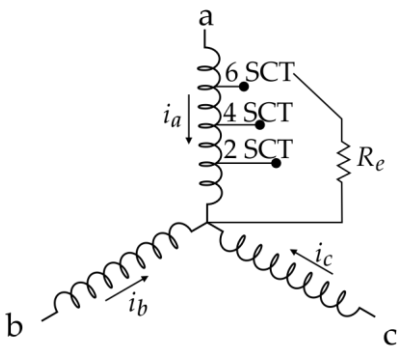

Figure 4. Schematic representation of the different severities of the ITSC fault.

The proposed method considers the use of three different physical magnitudes: vibrations, stator currents and stray-flux. The vibration signals are measured using a three axes accelerometer (LIS3LL02AS4) that is configured to work in the range of ±6 g. This sensor is located at the top of the IM as shown in Figure 5, the measurement of vibration belongs to the perpendicular plane of the IM axis (radial and tangential axes). Additionally, to carry out the stator current measurements, three hall-effect sensors L08P050D15 are placed in the power lines that go from the VFD to the IM. Finally, a proprietary board that uses hall sensors A1325 from ALLEGRO is used to obtain the IM stray flux. This board is also located on the top of the motor, next to the accelerometer as shown in Figure 5 and it can sense the radial flux and the axial flux simultaneously.

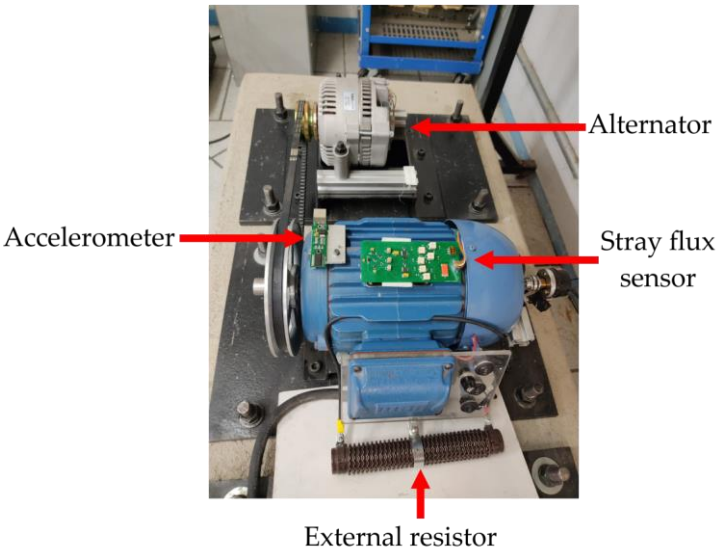

Figure 5. Main components of the experimental test bench.

All the data delivered by the sensors are collected using a proprietary data acquisition system (DAS) that is based on a field programmable gate array (FPGA) technology. The DAS includes two 4-channel analog-to-digital converters with 12-bit resolution (ADS7841 from Texas Instruments). This way, it is possible to acquire the occurrence of vibrations, the stator current consumption and the magnetic stray-flux in the IM at a single run; also, each acquired physical magnitude is acquired with a sampling frequency of 3000 Hz, 6000 Hz and 4000 Hz, respectively. During each performed test the aforementioned signals are collected during 150 seconds of the steady-state operation of the IM and then are sent to a personal computer where they are stored to be processed off-line.

4. Results and discussion

Preprints (www.preprints.org) | NOT PEER-REVIEWED | Posted: 2 June 2023 doi:10.20944/preprints202306.0180.v1

The proposed diagnosis methodology is validated under a real data set acquired from several experiments that are performed in a laboratory test bench, thus, as the proposed method describes, the acquisition of two vibrations signals (V_r and V_t), three stator currents signatures (C_1, C_2 and C_3) and two magnetic stray-flux signals (M_a and M_r) are continuously measured during the experimental evaluation of the healthy condition (HLT) and three incipient conditions of ITSC (2-SCTs, 4-SCTs and 6-SCTs). In addition, each one of the conditions under study is tested under different operating frequencies in the VFD (15 Hz, 30 Hz, 50 Hz and 60 Hz), consequently, during each test are acquired approximately 450 kSamples for each vibration signal, 900 kSamples for each stator current signature, and 600 kSamples for each magnetic stray flux signal.

Subsequently, the feature estimation is carried out in order to characterize the acquired signal for each performed test, in this regard, Equation (2) is applied to each one of the stored physical magnitudes in order to segment them in equal parts of one second; hence, for vibrations signals the length L used in Equation (2) is equal to $L_V = 3000$, meanwhile, L is equal to $L_C = 6000$ and $L_M = 4000$ for the stator currents and magnetic stray flux, respectively. Once the segmentation of the signals is accomplished, the estimation of the meaningful set of five statistical time domain features is individually estimated from each segmented part for each acquired signal. Then, for each studied condition is estimated a set of characteristic feature matrices $\mathbf{V_r}$, $\mathbf{V_t}$, $\mathbf{C_1}$, $\mathbf{C_2}$, $\mathbf{C_3}$, $\mathbf{M_a}$ and $\mathbf{M_r}$, where each feature matrix has five statistical features with 150 consecutive samples. Due to each condition under study is tested at different operating frequencies, a Global Feature Matrix (**GFM**) is generated for the HLT condition and for the three incipient conditions of ITSC (2-SCTs, 4-SCTs and 6-SCTs); thus, in such **GFM** are considered the pooling of all feature matrices for all physical magnitudes and all operating frequencies; i.e., the **GFM** for the HLT condition is generated following Equation (8) as $\mathbf{GFM_{HLT}}$, whereas $\mathbf{GFM_{2SCT}}$, $\mathbf{GFM_{4SCT}}$, $\mathbf{GFM_{6SCT}}$ are the **SCT** for the faulty conditions of 2-SCTs, 4-SCTs and 6-SCTs. It should be mentioned that each **GFM** is composed by 35 statistical time domain features estimated from different physical magnitudes with 600 consecutive samples, 150 samples per operating frequency.

$$\mathbf{GFM_{HLT}} = \begin{bmatrix} \boldsymbol{V_{r@15Hz}} & \boldsymbol{V_{t@15Hz}} & \boldsymbol{C_{1@15Hz}} & \boldsymbol{C_{2@15Hz}} & \boldsymbol{C_{3@15Hz}} & \boldsymbol{M_{a@15Hz}} & \boldsymbol{M_{r@15Hz}} \\ \boldsymbol{V_{r@30Hz}} & \boldsymbol{V_{t@30Hz}} & \boldsymbol{C_{1@30Hz}} & \boldsymbol{C_{2@30Hz}} & \boldsymbol{C_{3@30Hz}} & \boldsymbol{M_{a@30Hz}} & \boldsymbol{M_{r@30Hz}} \\ \boldsymbol{V_{r@50Hz}} & \boldsymbol{V_{t@50Hz}} & \boldsymbol{C_{1@50Hz}} & \boldsymbol{C_{2@50Hz}} & \boldsymbol{C_{3@50Hz}} & \boldsymbol{M_{a@50Hz}} & \boldsymbol{M_{r@50Hz}} \\ \boldsymbol{V_{r@60Hz}} & \boldsymbol{V_{t@60Hz}} & \boldsymbol{C_{1@60Hz}} & \boldsymbol{C_{2@60Hz}} & \boldsymbol{C_{3@60Hz}} & \boldsymbol{M_{a@60Hz}} & \boldsymbol{M_{r@60Hz}} \end{bmatrix}$$

Next, the **GFMs** for all considered conditions are then subjected to the dimensionality reduction procedure through the application of the LDA technique, thereby, the **GFMs** are then grouped following Equation (9) and during the reduction procedure is performed a space transformation from $\mathbb{R}^{(35)}$ to $\mathbb{R}^{(2)}$. Consequently, the use of the LDA allows the visualization of all considered conditions into a 2D plane, in Figure 6 is shown the resulting projection in which it is possible to appreciate that all studied conditions appear separated from each other. Additionally, it must be highlighted that the extracted features (Feature 1 and Feature 2) that are projected into the 2D plane also represent the linear combination, in different weights, of all considered features. In this regard, in Table 3 are summarized the weights assigned by the LDA during the feature reduction process, from Table 3 it can be analyzed the importance and contribution of each estimated feature; precisely, large absolute values mean a high-importance whereas small absolute values can be understood as non-relevant features.

Preprints (www.preprints.org) | NOT PEER-REVIEWED | Posted: 2 June 2023 doi:10.20944/preprints202306.0180.v1

$$\mathbf{X} = \begin{bmatrix} \mathbf{GFM_{HLT}} \\ \hline \mathbf{GFM_{2SCT}} \\ \hline \mathbf{GFM_{4SCT}} \\ \hline \mathbf{GFM_{6SCT}} \end{bmatrix}$$

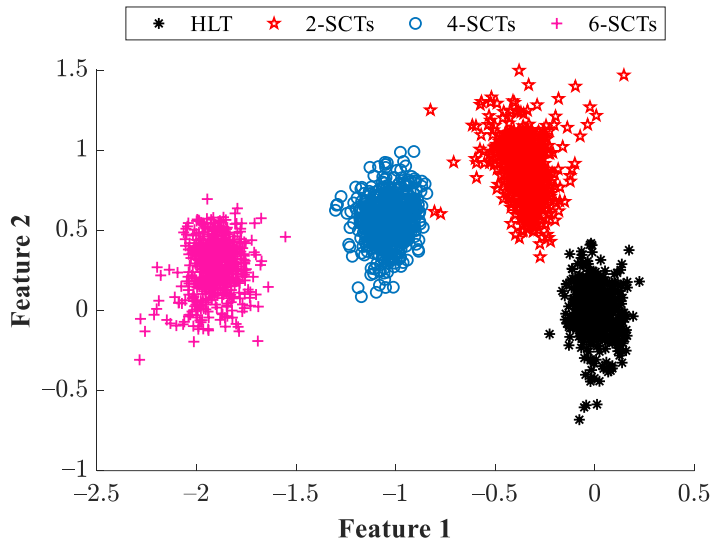

Figure 6. Visual representation achieved by the LDA technique into 2D plane when considering the vibration signals, stator currents and magnetic stray-flux for all considered conditions.

Table 3. Weights assigned by the LDA during the feature reduction procedure when transforming the original feature space ($\mathbb{R}^{(35)}$) into a lower space ($\mathbb{R}^{(2)}$).

Physical magnitude	**Projected feature**	Maximum value ($\hat{x}$)	Root mean square (RMS)	Standard deviation (σ)	Shape Factor (SF)	Crest Factor(CF)
Vibration (V_r)	**Feature 1**	-0.1332	0.0495	-0.0073	-0.0060	0.1320
	Feature 2	-0.2201	0.0257	0.0350	0.0220	0.2133
Vibration (V_t)	**Feature 1**	0.4306	0.0380	-0.0221	0.0047	-0.4204
	Feature 2	-0.4763	0.0566	-0.4186	0.3326	0.4828
Current (C_1)	**Feature 1**	-0.3922	0.0395	-0.0321	0.0185	0.3900
	Feature 2	-0.1997	0.0500	0.0217	-0.0188	0.2023
Current (C_2)	**Feature 1**	-0.3085	0.0485	-0.0495	0.0124	0.3104
	Feature 2	0.1472	0.0361	-0.0669	-0.0147	-0.1489
Current (C_3)	**Feature 1**	0.2123	0.0295	0.0176	0.0144	-0.2065
	Feature 2	-0.0175	-0.0943	-0.0196	-0.0064	0.0241
Stray-flux (M_a)	**Feature 1**	-0.0217	-0.0110	0.0388	-0.0005	0.0139
	Feature 2	0.0200	0.0064	0.0122	0.0010	-0.0085
Stray-flux (M_r)	**Feature 1**	-0.0251	-0.0147	0.0074	-0.0143	0.0191
	Feature 2	-0.0551	0.0316	0.0673	-0.0107	0.0345

Later, the extracted features by the LDA technique are then evaluated under a five-fold cross-validation scheme through the proposed NN-based classifier with the aim of carrying out the final diagnosis outcome; thereby, for each considered condition, 480 samples are used for training purposes and 120 samples are used for validation purposes. The training of the NN is achieved under a back-propagation approach during 70 epochs and, as an activation function is used a sigmoid function. Hence, the global classification ratio achieved during the training is 100%, whereas, a 99.4 % is reached during the validation;

Preprints (www.preprints.org) | NOT PEER-REVIEWED | Posted: 2 June 2023 doi:10.20944/preprints202306.0180.v1

in addition, in Table 4 are summarized the individual classifications. From Table 4 it can be appreciated that the proposed methodology leads to a high-performance classification avoiding positive falses which is a critical issue that may lead to the machine breakdown. On the other side, the use of the proposed NN classifier also facilitates the estimation of the decision regions on the 2*D* plane, hence, the decision regions for each tested conditions are shown in Figure 7, from the modeled classification regions in Figure 7 it can be observed that a specific regions has been assigned for each particular condition and, the assessment of new or unknown samples can be carried out in order to determinate the actual condition of IMs that suddenly operates under ITSC.

Table 4. Achieved classification ratios through the proposed NN-based classifier for the evaluation the extracted features by the LDA for all assessed conditions.

	True Class							
	Training				Test			
Assigned class	**Healthy**	**2-SCTs**	**4-SCTs**	**6-SCTs**	**Healthy**	**2-SCTs**	**4-SCTs**	**6-SCTs**
Healthy	480	0	0	0	120	0	0	0
2-SCTs	0	480	0	0	0	117	0	0
4-SCTs	0	0	480	0	0	3	120	0
6-SCTs	0	0	0	480	0	0	0	120

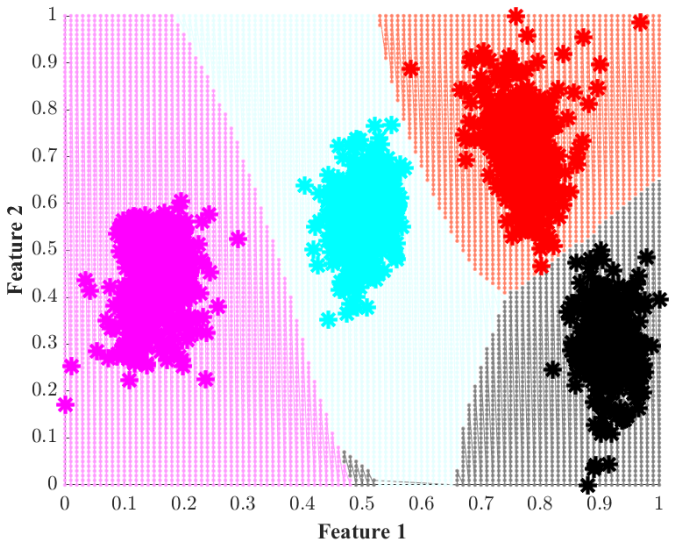

Figure 7. Resulting decision regions carried out by the proposed NN-based classifier when the 2*D* extracted features are evaluated.

Finally, in order to highlight that the use of different physical magnitudes such as vibrations, stator currents and magnetic stray-flux leads to an accurate detection of incipient ITSCs in IMs, the characteristic feature matrices estimated from different signals are combined between them whit the objective of analyze their performance. In this regard, a first combination considers only vibrations and stator currents, in a second combination are used vibrations and magnetic stray-flux and, the third combination includes stator currents with magnetic stray-flux. Then, each one of these combinations are subjected to the feature reduction procedure through the LDA and the resulting 2*d* projections are shown from Figure 8a to Figure 8c, respectively for each combination. As appreciated, the most critical case is when vibrations and magnetic stray-flux are combined since samples of all considered conditions appear to overlap between them; on the other hand, an improvement is obtained when the combinations of vibrations and stator currents as well as stator currents with magnetic stray-flux; however, for these combinations, the classifier may produce misclassifications between the HLT and 2-SCTs conditions. To finish the validation, the extracted features from Figure 8a to Figure 8c are also evaluated under the

Preprints (www.preprints.org) | NOT PEER-REVIEWED | Posted: 2 June 2023 doi:10.20944/preprints202306.0180.v1

same NN structure and the global classification rations achieved during the training and validations are summarized in Table 5. The obtained results show that this proposal can lead to an accurate identification of ITSCs in IMs, moreover, the characterization of vibrations, stator currents and magnetic stray-flux by means of statistical features offers a trade-off between simplicity efficiency when trends and changes are modeled from raw time-domain signals.

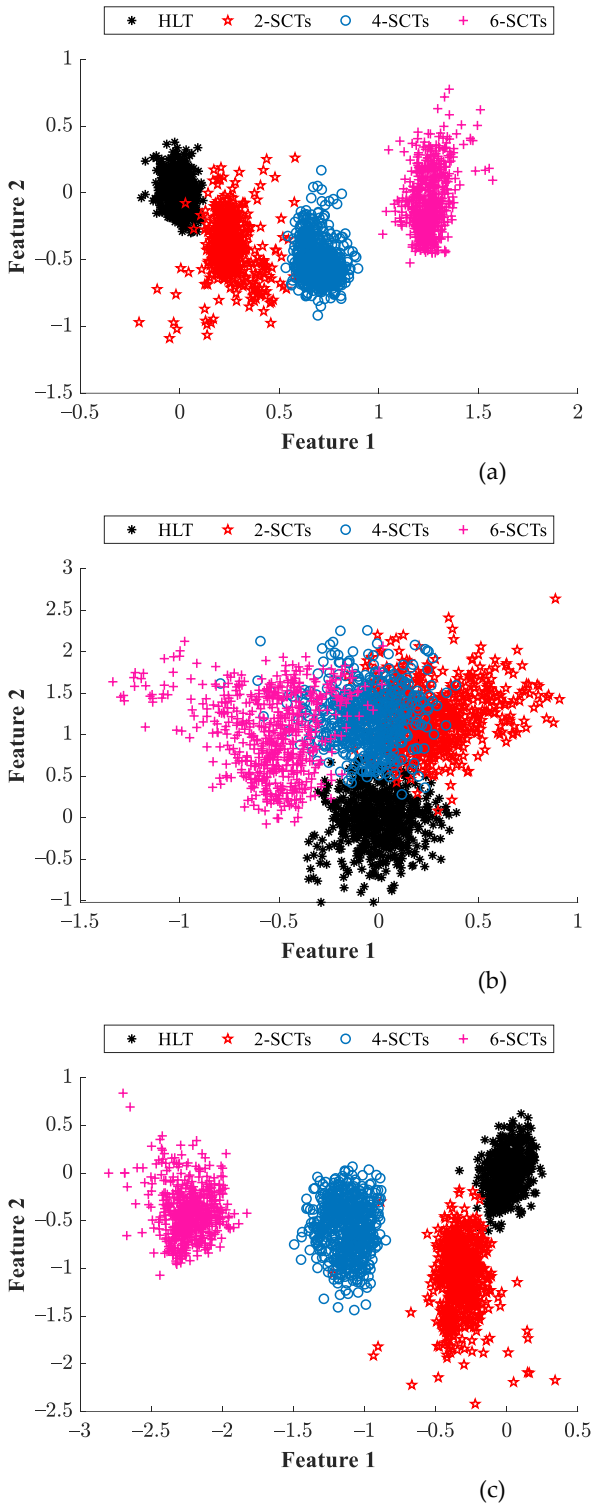

Figure8. *2D* projection achieved by the LDA technique when the physical magnitudes are combined as a) **vibrations + stator currents**, b) **vibrations + magnetic stray-flux** and c) **stator currents + magnetic stray-flux**.

 doi:10.20944/preprints202306.0180.v1

Table 5. Achieved classification ratios performed by the proposed NN-based classifier when different combinations of physical magnitudes are considered.

Considered approach	Training	Test
Vibrations + stator currents	92.7%	86.7%
Vibrations + magnetic stray-flux	86.0%	82.7%
Stator currents + magnetic stray-flux	98.4%	96.9%
Proposed approach: Vibrations + stator currents + magnetic stray-flux	100%	99.4%

5. Conclusions

The ITSC are common faults in IMs and they can produce catastrophic damage with consequences not only on the machinery but also in the safety of the personnel in the surroundings. Therefore, the development of strategies and methodologies for the proper identification of these faults becomes important for the industrial sector. In this sense, this work presented an approach based on data fusion and statistical machine learning that allows to address the occurrence of ITSC and it is also capable of identifying different severities of these faults. While most of the methodologies reported so far only use simulated signals, in this work is carried out experimentation with real signals from an induction motor with different damage severities. The results show that the selection of the physical variables to be used for the detection of the fault is not a trivial task. In this sense, the fusion of vibration, stator current, and magnetic stray flux data improves the results compared with the use of only one or two of these magnitudes. This situation results in a detection accuracy higher than 98%, proving that the proposed methodology is a helpful and reliable tool for identifying and classifying ITSC faults in IM. Moreover, it is worth noting that one of the major drawbacks of the machine learning approaches relies on the use of big amounts of data, a situation that results in complex processing and classification tasks that require a high computational burden. To overcome this issue, in this work is used the LDA technique to perform a dimensionality reduction, projecting all the data in a 2-dimensional space without losing relevant information. This way, it is possible to implement a simple classifier based on artificial neural networks.

Author Contributions: Conceptualization, J.J.S.-D., A.Y.J.-C., and D.A.E.-O.; methodology, A.Y.J-C. and D.A.E.-O.; software, J.J.S.-D.; validation, J.J.S.-D., A.Y.J.-C., and D.A.E.-O.; formal analysis, J.J.S.-D.; investigation, A.Y.J.-C.; resources, J.J.S.-D.; data curation, D.A.E.-O.; writing—original draft preparation, A.Y.J.-C.; writing—review and editing, A.Y.J.-C.; visualization, D.A.E.-O.; supervision, A.Y.J.-C. and J.J.S.-D.; project administration, J.J.S.-D.; funding acquisition, J.J.S.-D. All authors have read and agreed to the published version of the manuscript.

Funding: This project has been partially supported by "Fondo para el Desarrollo del Conocimiento" (FONDEC-UAQ-2022) under project number 20205007071601.

Conflicts of Interest: The authors declare no conflict of interest.

 doi:10.20944/preprints202306.0180.v1

References

1. Hajoary, P.K. Industry 4.0 Maturity and Readiness- A Case of a Steel Manufacturing Organization. *Procedia Computer Science* **2023**, *217*, 614–619, doi:10.1016/j.procs.2022.12.257.
2. Faheem, M.; Fizza, G.; Ashraf, M.W.; Butt, R.A.; Ngadi, Md.A.; Gungor, V.C. Big Data Acquired by Internet of Things-Enabled Industrial Multichannel Wireless Sensors Networks for Active Monitoring and Control in the Smart Grid Industry 4.0. *Data in Brief* **2021**, *35*, 106854, doi:10.1016/j.dib.2021.106854.
3. Soori, M.; Arezoo, B.; Dastres, R. Internet of Things for Smart Factories in Industry 4.0, a Review. *Internet of Things and Cyber-Physical Systems* **2023**, *3*, 192–204, doi:10.1016/j.iotcps.2023.04.006.
4. Singh, A.; Grant, B.; DeFour, R.; Sharma, C.; Bahadoorsingh, S. A Review of Induction Motor Fault Modeling. *Electric Power Systems Research* **2016**, *133*, 191–197, doi:10.1016/j.epsr.2015.12.017.
5. Torrent, M.; Blanqué, B.; Monjo, L. Replacing Induction Motors without Defined Efficiency Class by IE Class: Example of Energy, Economic, and Environmental Evaluation in 1.5 KW—IE3 Motors. *Machines* **2023**, *11*, 567, doi:10.3390/machines11050567.
6. Liang, H.; Chen, Y.; Liang, S.; Wang, C. Fault Detection of Stator Inter-Turn Short-Circuit in PMSM on Stator Current and Vibration Signal. *Applied Sciences* **2018**, *8*, 1677, doi:10.3390/app8091677.
7. Garcia-Calva, T.; Morinigo-Sotelo, D.; Fernandez-Cavero, V.; Romero-Troncoso, R. Early Detection of Faults in Induction Motors—A Review. *Energies* **2022**, *15*, 7855, doi:10.3390/en15217855.
8. Rangel-Magdaleno, J.; Peregrina-Barreto, H.; Ramirez-Cortes, J.; Cruz-Vega, I. Hilbert Spectrum Analysis of Induction Motors for the Detection of Incipient Broken Rotor Bars. *Measurement* **2017**, *109*, 247–255, doi:10.1016/j.measurement.2017.05.070.
9. Singh, G.; Anil Kumar, T.Ch.; Naikan, V.N.A. Efficiency Monitoring as a Strategy for Cost Effective Maintenance of Induction Motors for Minimizing Carbon Emission and Energy Consumption. *Reliability Engineering & System Safety* **2019**, *184*, 193–201, doi:10.1016/j.ress.2018.02.015.
10. Lu, S.-M. A Review of High-Efficiency Motors: Specification, Policy, and Technology. *Renewable and Sustainable Energy Reviews* **2016**, *59*, 1–12, doi:10.1016/j.rser.2015.12.360.
11. Ghosh, P.K.; Sadhu, P.K.; Basak, R.; Sanyal, A. Energy Efficient Design of Three Phase Induction Motor by Water Cycle Algorithm. *Ain Shams Engineering Journal* **2020**, *11*, 1139–1147, doi:10.1016/j.asej.2020.01.017.
12. Burgos Payán, M.; Roldan Fernandez, J.M.; Maza Ortega, J.M.; Riquelme Santos, J.M. Techno-Economic Optimal Power Rating of Induction Motors. *Applied Energy* **2019**, *240*, 1031–1048, doi:10.1016/j.apenergy.2019.02.016.
13. Kim, S.-H. Chapter 3 - Alternating Current Motors: Synchronous Motor and Induction Motor. In *Electric Motor Control*; Kim, S.-H., Ed.; Elsevier, 2017; pp. 95–152 ISBN 978-0-12-812138-2.
14. Skowron, M.; Wolkiewicz, M.; Orlowska-Kowalska, T.; Kowalski, C.T. Application of Self-Organizing Neural Networks to Electrical Fault Classification in Induction Motors. *Applied Sciences* **2019**, *9*, 616, doi:10.3390/app9040616.
15. Gangsar, P.; Tiwari, R. Signal Based Condition Monitoring Techniques for Fault Detection and Diagnosis of Induction Motors: A State-of-the-Art Review. *Mechanical Systems and Signal Processing* **2020**, *144*, 106908, doi:10.1016/j.ymssp.2020.106908.
16. Terron-Santiago, C.; Martinez-Roman, J.; Puche-Panadero, R.; Sapena-Bano, A. A Review of Techniques Used for Induction Machine Fault Modelling. *Sensors* **2021**, *21*, 4855, doi:10.3390/s21144855.
17. Faiz, J.; Keravand, M.; Ghasemi-Bijan, M.; Cruz, S.M.Â.; Bandar-Abadi, M. Impacts of Rotor Inter-Turn Short Circuit Fault upon Performance of Wound Rotor Induction Machines. *Electric Power Systems Research* **2016**, *135*, 48–58, doi:10.1016/j.epsr.2016.03.007.
18. Qiu, H.; Zhao, X.; Yang, C.; Ran, Y.; Wei, Y. Influence of Inter-Turn Short-Circuit Fault Considering Loop Current on Electromagnetic Field of High-Speed Permanent Magnet Generator with Gramme Ring Windings. *J. Electr. Eng. Technol.* **2019**, *14*, 701–710, doi:10.1007/s42835-019-00122-z.
19. Pietrowski, W.; Górny, K. Analysis of Torque Ripples of an Induction Motor Taking into Account a Inter-Turn Short-Circuit in a Stator Winding. *Energies* **2020**, *13*, 3626, doi:10.3390/en13143626.

20. Ullah, Z.; Hur, J. A Comprehensive Review of Winding Short Circuit Fault and Irreversible Demagnetization Fault Detection in PM Type Machines. *Energies* **2018**, *11*, 3309, doi:10.3390/en11123309.
21. Moosavi, S.-M.M.; Faiz, J.; Abadi, M.B.; Cruz, S.M.A. Comparison of Rotor Electrical Fault Indices Owing to Inter-Turn Short Circuit and Unbalanced Resistance in Doubly-Fed Induction Generator. *IET Electric Power Applications* **2019**, *13*, 235–242, doi:10.1049/iet-epa.2018.5528.
22. Forstner, G.; Kugi, A.; Kemmetmüller, W. Fault-Tolerant Torque Control of a Three-Phase Permanent Magnet Synchronous Motor with Inter-Turn Winding Short Circuit. *Control Engineering Practice* **2021**, *113*, 104846, doi:10.1016/j.conengprac.2021.104846.
23. Adouni, A.; J. Marques Cardoso, A. Thermal Analysis of Low-Power Three-Phase Induction Motors Operating under Voltage Unbalance and Inter-Turn Short Circuit Faults. *Machines* **2021**, *9*, 2, doi:10.3390/machines9010002.
24. Yuan, X.-H.; He, Y.-L.; Liu, M.-Y.; Wang, H.; Wan, S.-T.; Vakil, G. Impact of the Field Winding Interturn Short-Circuit Position on Rotor Vibration Properties in Synchronous Generators. *Mathematical Problems in Engineering* **2021**, *2021*, e9236726, doi:10.1155/2021/9236726.
25. Yang, J.; Dou, M.; Dai, Z. Modeling and Fault Diagnosis of Interturn Short Circuit for Five-Phase Permanent Magnet Synchronous Motor. *Journal of Electrical and Computer Engineering* **2015**, *2015*, e168786, doi:10.1155/2015/168786.
26. He, Y.-L.; Xu, M.-X.; Zhang, W.; Wang, X.-L.; Lu, P.; Gerada, C.; Gerada, D. Impact of Stator Interturn Short Circuit Position on End Winding Vibration in Synchronous Generators. *IEEE Transactions on Energy Conversion* **2021**, *36*, 713–724, doi:10.1109/TEC.2020.3021901.
27. Im, S.-H.; Gu, B.-G. Study of Induction Motor Inter-Turn Fault Part I: Development of Fault Models with Distorted Flux Representation. *Energies* **2022**, *15*, 894, doi:10.3390/en15030894.
28. Ghanbari, T.; Mehraban, A.; Farjah, E. Inter-Turn Fault Detection of Induction Motors Using a Method Based on Spectrogram of Motor Currents. *Measurement* **2022**, *205*, 112180, doi:10.1016/j.measurement.2022.112180.
29. Irhoumah, M.; Pusca, R.; Lefevre, E.; Mercier, D.; Romary, R. Detection of the Stator Winding Inter-Turn Faults in Induction and Synchronous Machines through the Correlation Between Harmonics of the Voltage of Two Magnetic Flux Sensors. *IEEE Transactions on Industry Applications* **2019**, *55*, doi:10.1109/TIA.2019.2899560.
30. Ehya, H.; Nysveen, A. Pattern Recognition of Interturn Short Circuit Fault in a Synchronous Generator Using Magnetic Flux. *IEEE Transactions on Industry Applications* **2021**, *57*, 3573–3581, doi:10.1109/TIA.2021.3072881.
31. Liu, X.; Miao, W.; Xu, Q.; Cao, L.; Liu, C.; Pong, P.W.T. Inter-Turn Short-Circuit Fault Detection Approach for Permanent Magnet Synchronous Machines Through Stray Magnetic Field Sensing. *IEEE Sensors Journal* **2019**, *19*, 7884–7895, doi:10.1109/JSEN.2019.2918018.
32. Zorig, A.; Hedayati Kia, S.; Chouder, A.; Rabhi, A. A Comparative Study for Stator Winding Inter-Turn Short-Circuit Fault Detection Based on Harmonic Analysis of Induction Machine Signatures. *Mathematics and Computers in Simulation* **2022**, *196*, 273–288, doi:10.1016/j.matcom.2022.01.019.
33. Maraaba, L.S.; Twaha, S.; Memon, A.; Al-Hamouz, Z. Recognition of Stator Winding Inter-Turn Fault in Interior-Mount LSPMSM Using Acoustic Signals. *Symmetry* **2020**, *12*, 1370, doi:10.3390/sym12081370.
34. Eftekhari, M.; Moallem, M.; Sadri, S.; Hsieh, M.-F. A Novel Indicator of Stator Winding Inter-Turn Fault in Induction Motor Using Infrared Thermal Imaging. *Infrared Physics & Technology* **2013**, *61*, 330–336, doi:10.1016/j.infrared.2013.10.001.
35. Singh, G.; Anil Kumar, T.Ch.; Naikan, V.N.A. Induction Motor Inter Turn Fault Detection Using Infrared Thermographic Analysis. *Infrared Physics & Technology* **2016**, *77*, 277–282, doi:10.1016/j.infrared.2016.06.010.
36. Kumar, P.S.; Xie, L.; Halick, M.S.M.; Vaiyapuri, V. Stator End-Winding Thermal and Magnetic Sensor Arrays for Online Stator Inter-Turn Fault Detection. *IEEE Sensors Journal* **2021**, *21*, 5312–5321, doi:10.1109/JSEN.2020.3029041.
37. Wu, Y.-H.; Liu, M.-Y.; Song, H.; Li, C.; Yang, X.-L. A Temperature and Magnetic Field-Based Approach for Stator Inter-Turn Fault Detection. *IEEE Sensors Journal* **2022**, *22*, 17799–17807, doi:10.1109/JSEN.2022.3198146.

38. Xu, Z.; Hu, C.; Yang, F.; Kuo, S.-H.; Goh, C.-K.; Gupta, A.; Nadarajan, S. Data-Driven Inter-Turn Short Circuit Fault Detection in Induction Machines. *IEEE Access* **2017**, *5*, 25055–25068, doi:10.1109/ACCESS.2017.2764474.
39. Chen, Z.; Liang, D.; Jia, S.; Yang, L.; Yang, S. Incipient Interturn Short Circuit Fault Diagnosis of Permanent Magnet Synchronous Motors Based on the Data-Driven Digital Twin Model. *IEEE Journal of Emerging and Selected Topics in Power Electronics* **2023**, 1–1, doi:10.1109/JESTPE.2023.3255249.
40. Shih, K.-J.; Hsieh, M.-F.; Chen, B.-J.; Huang, S.-F. Machine Learning for Inter-Turn Short-Circuit Fault Diagnosis in Permanent Magnet Synchronous Motors. *IEEE Transactions on Magnetics* **2022**, *58*, 1–7, doi:10.1109/TMAG.2022.3169173.
41. Guerreiro Carvalho Cunha, R.; da Silva, E.T.; Marques de Sá Medeiros, C. Machine Learning and Multiresolution Decomposition for Embedded Applications to Detect Short-Circuit in Induction Motors. *Computers in Industry* **2021**, *129*, 103461, doi:10.1016/j.compind.2021.103461.
42. Liang, S.; Chen, Y.; Liang, H.; Li, X. Sparse Representation and SVM Diagnosis Method for Inter-Turn Short-Circuit Fault in PMSM. *Applied Sciences* **2019**, *9*, 224, doi:10.3390/app9020224.
43. Ehya, H.; Skreien, T.N.; Nysveen, A. Intelligent Data-Driven Diagnosis of Incipient Interturn Short Circuit Fault in Field Winding of Salient Pole Synchronous Generators. *IEEE Transactions on Industrial Informatics* **2022**, *18*, 3286–3294, doi:10.1109/TII.2021.3054674.
44. Li, Y.; Wang, Y.; Zhang, Y.; Zhang, J. Diagnosis of Inter-Turn Short Circuit of Permanent Magnet Synchronous Motor Based on Deep Learning and Small Fault Samples. *Neurocomputing* **2021**, *442*, 348–358, doi:10.1016/j.neucom.2020.04.160.
45. Maraaba, L.; Al-Hamouz, Z.; Abido, M. An Efficient Stator Inter-Turn Fault Diagnosis Tool for Induction Motors. *Energies* **2018**, *11*, 653, doi:10.3390/en11030653.
46. Duda, R.O.; Hart, P.E.; Stork, D.G. *Pattern Classification*; 2nd ed.; Wiley: New York, 2001; ISBN 978-0-471-05669-0.